

Enhanced strength and ductility of friction stir processed Cu–Al alloys with abundant twin boundaries

P. Xue, B.L. Xiao and Z.Y. Ma*

Shenyang National Laboratory for Materials Science, Institute of Metal Research, Chinese Academy of Sciences, 72 Wenhua Road, Shenyang 110016, People's Republic of China

Received 6 November 2012; revised 29 December 2012; accepted 1 January 2013

Available online 10 January 2013

Ultrafine-grained Cu–Al alloys were prepared via friction stir processing (FSP) with additional rapid cooling. These FSP Cu–Al alloys exhibited equiaxed recrystallized grains with relatively low dislocation density and a high fraction (96%) of high-angle grain boundaries. Abundant annealing twin boundaries were successfully introduced into the ultrafine grains in FSP Cu–15Al (at.%) alloy, resulting in superior strength–ductility synergy with a yield strength of ~ 700 MPa and a uniform elongation of $\sim 13\%$. © 2013 Acta Materialia Inc. Published by Elsevier Ltd. All rights reserved.

Keywords: Copper alloys; Twin boundaries; Friction stir processing; Ultrafine grains; Ductility

Nanostructured (NS) and ultrafine-grained (UFG) materials have attracted considerable interest due to their special microstructure and mechanical properties [1,2]. Numerous investigations have showed that although NS and UFG materials exhibit very high strength or hardness, they are of very low ductility or even brittle, resulting in insuperable problems for structural applications [3–8]. The disappointingly low ductility can be attributed to processing artifacts, plastic instability with little or no strain hardening (dislocation storage) capacity, and low resistance to crack initiation and propagation [4].

Recently, a variety of strategies aimed at improving the poor ductility of the NS and UFG materials were summarized by Zhao et al. [9]. Among these strategies, introducing abundant coherent twin boundaries (TBs) in the ultrafine grains is an effective method of improving strength and ductility simultaneously [10,11]. TBs within grains can be introduced during processing (so-called growth twins), plastic deformation (deformation twins) or recrystallization of deformed structures upon annealing (annealing twins) [11]. Copious nanoscale coherent growth TBs have been successfully introduced into ultrafine Cu grains by Lu et al. [10] via pulsed electrodeposition, resulting in superior tensile properties.

Unfortunately, this deposition process could only produce thin foils, limiting its practical engineering applications.

Compared to the deposition processes, various severe plastic deformation (SPD) methods provide practical approaches to introducing TBs into bulk metal and alloy samples [1]. A high density of deformation TBs can be introduced in pure Cu by dynamic plastic deformation (DPD) at high strain rate and low temperature [7]. Furthermore, by adding alloy elements (Al, Zn) to decrease the stacking fault energy (SFE), abundant deformation TBs can also be introduced into UFG Cu alloys by equal-channel angular pressing (ECAP) and high-pressure torsion (HPT) methods [12–16]. However, a high density of dislocations usually existed in these ultrafine grains and on the deformation TBs, and there was little or no room for further accumulation of dislocations. Therefore, insufficient strain hardening was also achieved in these UFG Cu and alloys, resulting in very low ductility [11–16].

Subsequent annealing after SPD provides an effective method of enhancing the strain hardening of UFG materials due to the reduced dislocation density and the coarsened grains generated during recrystallization [17–19]. Hence, enhanced strength–ductility synergy was usually achieved in these annealed SPD Cu and alloys. However, these two-step methods are not convenient in practical application, and the annealing process is not easily controlled due to the strong driving force

* Corresponding author. Tel./fax: +86 24 83978908; e-mail: zyrna@imr.ac.cn

toward recrystallization after SPD. Generally, the strength is greatly reduced when the desirable ductility is achieved [19].

A new simple processing technique, friction stir processing (FSP), was recently developed as a method for achieving microstructural modification [20]. FSP with additional rapid cooling has been demonstrated to be an effective method of preparing bulk NS and UFG materials, such as pure Cu, Al and Mg alloys [21–23]. During FSP, a combination of SPD and relatively high temperature is achieved, similar to that of SPD and a subsequent annealing process. By decreasing the SFE, it is expected that abundant annealing TBs can be introduced into the ultrafine grains via a dynamic recrystallization (DRX) process in FSP Cu alloys. Therefore, this study aims to investigate whether enhanced strength and ductility can be achieved in FSP Cu alloys by introducing abundant TBs.

Two Cu–Al alloys with low SFEs (Cu–5 at.% Al: $\sim 28 \text{ mJ m}^{-2}$; Cu–15 at.% Al: $\sim 6 \text{ mJ m}^{-2}$) were used in this study. To yield a low heat input, the Cu–Al alloy plates, which were 4 mm thick, were first fixed in water and then subjected to FSP at a rotation rate of 600 rpm and a traverse speed of 50 mm min^{-1} using a tool with a shoulder 12 mm in diameter. During FSP, additional rapid cooling by flowing water was adopted.

Microstructural examination was completed using transmission electron microscopy (TEM) and electron backscatter diffraction (EBSD). EBSD scans were performed using an Oxford HKL Channel 5 system on a LEO Supra 35 FEG scanning electron microscope with a step size of 70 nm. The dog-bone-shaped tensile specimens with a gauge length of 8 mm and a width of 2 mm were machined along the processing direction from the processed zone and polished to a thickness of $\sim 1 \text{ mm}$. Uniaxial tensile tests were conducted at room temperature at an initial strain rate of $1 \times 10^{-3} \text{ s}^{-1}$. The displacement of the gauge section was measured using a laser extensometer with an accuracy of $1 \mu\text{m}$.

Figure 1 shows the microstructural characteristics of the FSP Cu–Al alloys observed by EBSD. Both FSP Cu–Al alloys were composed of ultrafine grains with a typical equiaxed recrystallized microstructure (Fig. 1a and b). It is clear that the grains were refined as the SFE decreased, and the average grain sizes estimated by EBSD, without considering TBs, were about 600 and 500 nm for FSP Cu–5Al and Cu–15Al alloys, respectively. Considering all grain boundary misorientation angles $>2^\circ$, the high-angle grain boundaries (HAGBs, misorientation angle $\geq 15^\circ$) in the FSP Cu–5Al and Cu–15Al alloys comprised about 87% and 96% of the total grain boundary length, respectively (Fig. 1c and d). These fractions are obviously larger than that of SPD Cu alloys, which have a HAGB fraction of $\sim 62\%$ even after complex procedures [15]. Compared with the random distribution for a cubic polycrystal and ECAP Cu–Al alloys [15], the FSP Cu–Al alloys exhibited one large peak at $\sim 60^\circ$, which resulted from the $\Sigma 3$ TBs. As the SFE decreased, the fraction of the 60° peak increased from $\sim 4\%$ in the FSP Cu–5Al alloy to $\sim 13\%$ in the FSP Cu–15Al alloy. This indicates that more TBs were introduced into the FSP UFG Cu–Al alloys by decreasing the SFE.

The TEM bright-field images in Figure 2a and b showed that the UFG microstructure of the FSP Cu–Al alloys was characterized by equiaxed grains and a relatively low density of dislocations. In addition to the ultrafine grains, some relatively coarse micrograins (1–2 μm) were also observed in both FSP Cu–Al alloys (Figs. 1a,b and 2c), and the number was larger in the FSP Cu–5Al alloy. When the Al content was relatively low (5 at.%), only a single TB or TB layer was observed in the ultrafine grains (Fig. 2a), which was similar to that of FSP pure Cu [23]. However, as the Al content increased to 15 at.%, many TBs and TB layers were detected in the ultrafine grains (Fig. 2b). Even in the micrograins of FSP Cu–15Al alloy, abundant TBs and TB layers were also observed (Fig. 2c). The width of

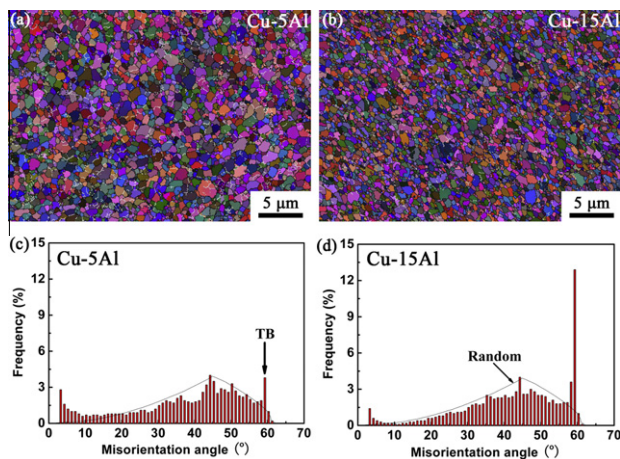


Figure 1. Representative EBSD images of (a) FSP Cu–5Al and (b) FSP Cu–15Al alloys; distribution of grain boundary misorientation angle for (c) FSP Cu–5Al and (d) FSP Cu–15Al alloys (the short dotted line represents a random misorientation distribution for a cubic polycrystal).

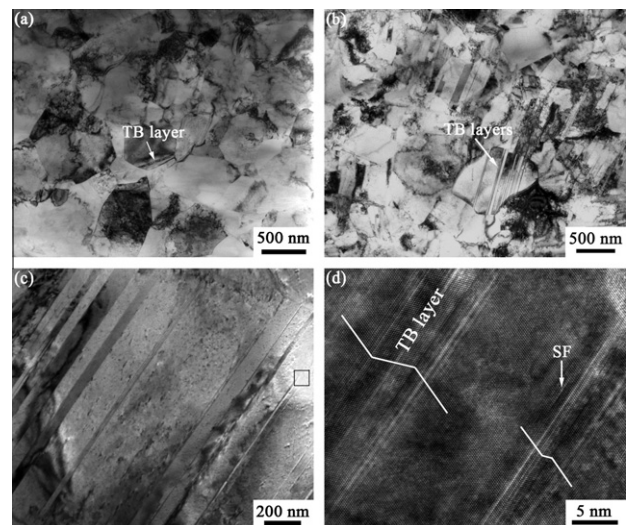


Figure 2. Typical bright-field TEM images of (a) FSP Cu–5Al, (b and c) FSP Cu–15Al, and (d) a typical high-resolution TEM image of TB layers in FSP Cu–15Al alloy.

the TB layers was refined to several nanometers, and few dislocations were detected in the ultrafine grains and on the TBs. Moreover, many stacking faults (SFs) were also observed in the FSP Cu–15Al alloy (Fig. 2d).

Unlike that for SPD materials, DRX should be the refinement mechanism for FSP materials [20–23], and this is confirmed by the equiaxed grain structure observed by EBSD and TEM. Grains in the FSP Cu–Al alloys should undergo growth after the formation of the initial grain units, and hence some relatively coarse micrograins were formed because preferential grain growth can occur at the appropriate strain state, temperature and misorientation during DRX [24]. Annealing twins can be generated during recrystallization and grain growth processes driven by minimization of the total excess energies of boundaries separating newly formed grains, and SFs produced by slip would act as nuclei for annealing twins [25,26]. Usually, the tendency towards the generation of deformation twins increases as the SFE decreases [11–15], and the same is true for annealing twins [27,28]; therefore abundant annealing TBs were introduced in the FSP Cu–15Al alloy with a very low SFE.

Similar to the coherent growth TBs, few dislocations were observed on the annealing TBs (Fig. 2d), and these TBs differ structurally from the deformation TBs, on which a high density of dislocations is usually detected [11]. The existence of a high density of dislocations can change the intrinsic TB structure in the deformation TBs, and this may be the reason why no obvious peak of TBs (~60°) was observed from the distribution of grain boundary misorientation angles by EBSD in SPD Cu alloys [15].

The true tensile stress–strain curves of the FSP Cu–Al alloys, as well as the coarse-grained (CG) reference Cu–Al alloys, are compared in Figure 3a. CG Cu–5Al and Cu–15Al alloys exhibited low values of yield strength (YS) of ~65 and ~80 MPa, respectively. After FSP, it was apparent that the YS increased significantly to about 400 and 700 MPa for the FSP Cu–5Al and Cu–15Al alloys, respectively. More importantly, both FSP Cu–Al alloys showed continuous strain hardening to significant strains, and this can enhance the tensile ductility. Strain hardening is very important for NS and UFG materials because the onset of plastic instability (necking or shear localization) in tension is governed by the Considère criterion:

$$\left(\frac{\partial\sigma}{\partial\varepsilon}\right)_i \leq \sigma, \quad (1)$$

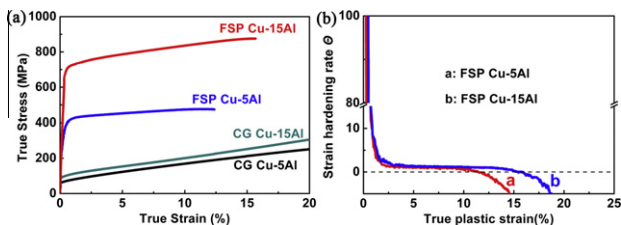


Figure 3. (a) Tensile true stress–strain curves of FSP and CG Cu–Al alloys; (b) normalized strain hardening rate (Θ) vs. true strain of the FSP Cu–Al alloys.

where σ and ε are the true stress and true strain, respectively. The normalized strain hardening rate Θ , where $\Theta = \frac{1}{\sigma} \left(\frac{\partial\sigma}{\partial\varepsilon}\right)_i$, vs. the true strain of both FSP Cu–Al alloys is shown in Figure 3b. It is clear that both FSP Cu–Al alloys exhibited positive strain hardening to significant strains. According to the Considère criterion, the values of uniform elongation (elongation before plastic instability, i.e. when $\Theta \geq 1$) were calculated to be ~9% and ~13% for FSP Cu–5Al and Cu–15Al alloys, respectively.

Figure 4 summarizes the experimental data on uniform elongation vs. YS for various Cu alloys prepared by FSP and SPD methods [12–15]. It is clear that all the results exhibited enhanced YS with decreases in the SFE. Meanwhile, the uniform elongation increased simultaneously in DPD, ECAP and FSP Cu alloys. However, the uniform elongation of HPT Cu alloys decreased slightly at high alloy contents. The uniform elongations of most SPD Cu alloys were <5%, which is below the criterion for structural applications. By contrast, a high uniform elongation of ~13% can be obtained in the FSP Cu–15Al alloy together with a very high YS of ~700 MPa, and this superior strength–ductility synergy should be attributed to its special microstructures.

It has been documented that the introduction of Al atoms into Cu matrix only leads to a weak solution-strengthening effect [12–15]. In the present study, the YS increment introduced by adding 15 at.% Al into the Cu matrix was only ~20 MPa for CG samples. On the other hand, the reduced grain size and the high density of TBs in the FSP Cu–15Al alloy made the equivalent grain size (containing TBs) decrease significantly, and this can greatly enhance the YS according to the Hall–Petch effect. In terms of ductility, the apparently enhanced uniform elongation of the FSP Cu–15Al alloy may be attributed to the following three factors.

First, the relatively low dislocation density due to the recrystallization process provides more room for further dislocation storage. Previous studies indicated that the tensile ductility could be enhanced in UFG materials with lower dislocation density, which can provide more room to store dislocations [9,17–19,23,29]. SPD UFG materials exhibited quite a high density of defects and relatively poor microstructure stability, resulting in easier dislocation saturation in subsequent plastic deformation, and therefore very low ductility was usually achieved [1–8,12–15]. Obviously, low dislocation density in the present FSP Cu–Al alloys allowed further

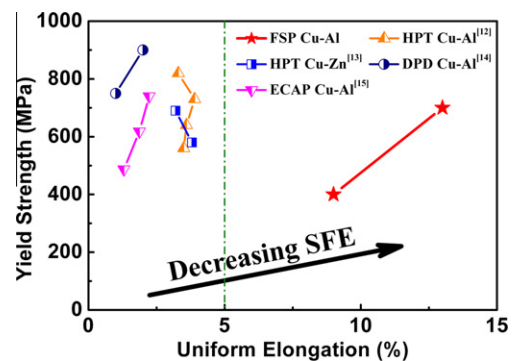


Figure 4. Relationship between uniform elongation and YS of the UFG Cu alloys prepared by FSP and various SPD methods [12–15].

accumulation of dislocations during tensile tests, and this led to the enhanced strain hardening and ductility.

Second, a high fraction of HAGBs is beneficial for enhancing the strain hardening. HAGBs hinder and block dislocations more effectively, which is conducive to increasing the strain-hardening capacity and improving the ductility [9,29]. Moreover, some trials have indicated that reasonable ductility could be obtained by HAGB sliding and related activities in UFG materials [9,30]. HAGB sliding leads to dislocation emissions at triple junctions owing to the presence of high stress concentrations, and these dislocations may act to increase the strain hardening [9,29,30].

Lastly, but most importantly, a TB-related mechanism can act during tensile deformation of an FSP Cu–15Al alloy with abundant annealing TBs. Similar to the coherent growth TBs, the presence of abundant annealing TBs provides adequate barriers to dislocation motion for strengthening and creates more local sites for nucleating and accommodating dislocations, thereby elevating ductility and strain hardening [10,11]. Furthermore, the thickness of most TB layers in the FSP Cu–15Al alloy was smaller than that of the growth TB layers and the deformation TB layers, whose thickness was usually <50 nm [10–15]. Therefore, an adequate driving force for further formation of deformation twins during tension still exists, according to previous studies [17,31]. This can help not only to accommodate the plastic deformation but also to improve the strain-hardening rate through a twinning-induced plasticity effect and thereby to further enhance the ductility [31].

In summary, the present results demonstrate that enhanced strength and ductility can be achieved in FSP Cu–15Al alloy. The microstructure was characterized by equiaxed ultrafine grains with a relatively low density of dislocations and a high fraction of HAGBs of as much as 96%. Superior strength–ductility synergy with a YS of ~700 MPa and a uniform elongation of ~13% was achieved in this FSP Cu–15Al alloy, a finding that was attributed mainly to the abundant annealing TBs introduced in the ultrafine grains.

This work was supported by the National Natural Science Foundation of China under Grant Nos. 51071150 and 50890171.

[1] R.Z. Valiev, Y. Estrin, Z. Horita, T.G. Langdon, M.J. Zehetbauer, Y.T. Zhu, JOM 58 (2006) 33.

- [2] M. Dao, L. Lu, R.J. Asaro, J.T.M. De Hosson, E. Ma, Acta Mater. 55 (2007) 4041.
- [3] C.C. Koch, D.G. Morris, K. Lu, A. Inoue, MRS Bull. 24 (1999) 54.
- [4] C.C. Koch, Scr. Mater. 49 (2003) 657.
- [5] Y.T. Zhu, X.Z. Liao, Nat. Mater. 3 (2004) 351.
- [6] F.D. Torre, R. Lapovok, J. Sandlin, P.F. Thomson, C.H.J. Davies, E.V. Pereloma, Acta Mater. 52 (2004) 4819.
- [7] W.S. Zhao, N.R. Tao, J.Y. Guo, Q.H. Lu, K. Lu, Scr. Mater. 53 (2005) 745.
- [8] Y.M. Wang, E. Ma, M.W. Chen, Appl. Phys. Lett. 80 (2002) 2395.
- [9] Y.H. Zhao, Y.T. Zhu, E.J. Lavernia, Adv. Eng. Mater. 12 (2010) 769.
- [10] L. Lu, Y. Shen, X. Chen, L. Qian, K. Lu, Science 304 (2004) 422.
- [11] K. Lu, L. Lu, S. Suresh, Science 324 (2009) 349.
- [12] X.H. An, Q.Y. Lin, S.D. Wu, Z.F. Zhang, R.B. Figueiredo, N. Gao, T.G. Langdon, Scr. Mater. 64 (2011) 954.
- [13] Y.H. Zhao, X.Z. Liao, Z. Horita, T.G. Langdon, Y.T. Zhu, Mater. Sci. Eng. A 493 (2008) 123.
- [14] Y. Zhang, N.R. Tao, K. Lu, Acta Mater. 59 (2011) 6048.
- [15] S. Qu, X.H. An, H.J. Yang, C.X. Huang, G. Yang, Q.S. Zang, Z.G. Wang, S.D. Wu, Z.F. Zhang, Acta Mater. 57 (2009) 1586.
- [16] Y.T. Zhu, X.Z. Liao, X.L. Wu, Prog. Mater. Sci. 57 (2012) 1.
- [17] X.H. An, S.D. Wu, Z.F. Zhang, R.B. Figueiredo, N. Gao, T.G. Langdon, Scr. Mater. 66 (2012) 227.
- [18] Y.S. Li, Y. Zhang, N.R. Tao, K. Lu, Scr. Mater. 59 (2008) 475.
- [19] Y.M. Wang, M.W. Chen, E. Ma, Nature 419 (2002) 912.
- [20] R.S. Mishra, Z.Y. Ma, Mater. Sci. Eng. R 50 (2005) 1.
- [21] J.Q. Su, T.W. Nelson, C.J. Sterling, Scr. Mater. 52 (2005) 135–140.
- [22] C.I. Chang, X.H. Du, J.C. Huang, Scr. Mater. 57 (2007) 209–212.
- [23] P. Xue, B.L. Xiao, Z.Y. Ma, Mater. Sci. Eng. A 532 (2012) 106.
- [24] D.J. Jensen, Acta Metall. Mater. 43 (1995) 4117.
- [25] J.E. Burke, D. Turnbull, Prog. Metal Phys. 3 (1952) 220.
- [26] S. Mahajan, C.S. Pande, M.A. Imam, B.B. Rath, Acta Mater. 45 (1997) 2633.
- [27] P.R. Thornton, T.E. Mitchell, Philos. Mag. 7 (1962) 361.
- [28] S. Dash, N. Brown, Acta Metall. 11 (1963) 1067.
- [29] Y.H. Zhao, J.F. Bingert, Y.T. Zhu, X.Z. Liao, R.Z. Valiev, Z. Horita, T.G. Langdon, Y.Z. Zhou, E.J. Lavernia, Appl. Phys. Lett. 92 (2008) 081903.
- [30] N.Q. Chinh, P. Szommer, Z. Horita, T.G. Langdon, Adv. Mater. 18 (2006) 34–39.
- [31] H.K.D.H. Bhadeshia, Scr. Mater. 66 (2012) 955.